Journal of Power Sources 234 (2013) 38–47

Contents lists available at SciVerse ScienceDirect

Journal of Power Sources

journal homepage: www.elsevier.com/locate/jpowsour

Mechanical properties of catalyst coated membranes for fuel cells

Marc-Antoni Goulet [a], Ramin M.H. Khorasany [a], Chris De Torres [a], Mike Lauritzen [b], Erik Kjeang [a,*], G. Gary Wang [a], Nimal Rajapakse [a]

[a] Mechatronic Systems Engineering, School of Engineering Science, Simon Fraser University, 250-13450 102 Avenue, Surrey, BC V3T 0A3, Canada
[b] Ballard Power Systems, 9000 Glenlyon Parkway, Burnaby, BC V5J 5J8, Canada

HIGHLIGHTS

- Tensile properties of catalyst coated membranes differ from those of pure membranes.
- Catalyst layers contribute mechanical reinforcement to the membrane.
- Catalyst layers also increase the contraction forces due to dehydration.
- The obtained properties are recommended for finite element analysis of fuel cells.

ARTICLE INFO

Article history:
Received 15 November 2012
Received in revised form
17 January 2013
Accepted 19 January 2013
Available online 28 January 2013

Keywords:
Polymer electrolyte membrane
Catalyst coated membrane
Fuel cell
Mechanical properties
Tensile test
Swelling

ABSTRACT

The change in mechanical properties of a catalyst coated membrane (CCM) as a function of humidity and temperature is investigated and compared to that of a pure perfluorosulfonic acid (PFSA) membrane at the same conditions. The results of tensile tests indicate that the modulus and yield stress of the CCM vary differently than those of the membrane with respect to temperature and humidity. Both materials decrease in stiffness and strength at higher temperature and humidity, but proportionally more so for the CCM leading to less desirable mechanical properties at typical fuel cell operating conditions. Length-wise swelling of the two materials during hydration is also investigated and is shown to be almost twice as great for the pure membrane material versus the CCM. The tensile forces induced by dehydration of constrained samples are also measured. The peak and residual dehydration forces are larger for the CCM compared to the membrane by a factor which occasionally exceeds the average reinforcement provided by the catalyst layers. These results emphasize the importance of the catalyst layers on the overall mechanical properties of the CCM and the need to consider them when attempting to model *in situ* stress distributions.

1. Introduction

In an effort to find sustainable zero-emission alternatives for the oil dominated transportation sector, a substantial amount of research has focused on hydrogen fuel cell technology due to its high power density and clean operation. Most low-temperature fuel cells for automotive applications currently rely on a polymer electrolyte membrane (PEM) to allow ionic conduction while separating the fuel and oxidant streams. Perfluorosulfonic acid (PFSA) is presently the material of choice for this function, with a hydrophobic chemically stable carbon backbone and a high density of sulfonic acid side-chains which form hydrophilic microscopic domains capable of hydrogen ion transport under hydrated conditions [1].

As with all energy conversion technologies, the primary design challenge for PEM fuel cells is to maximize efficiency and minimize cost of production. In order to reduce ohmic losses and cost, membrane thicknesses have decreased considerably over the past few years, which in turn have led to more durability issues [2]. Much of the initial research on PEM fuel cell durability was focused on chemical membrane degradation mechanisms induced by radical formation and attack [3]. In recent years however, it was also recognized that purely mechanical modes of membrane failure are possible due in large part to the cyclical hygrothermal stresses experienced by the membranes during fuel cell operation [2–4]. Several studies have shown that cycling between humidified and dry nitrogen gas streams accelerates mechanical degradation in a process akin to fatigue [4–7]. With progress being made toward reducing the chemically destructive reactions within the fuel cell, attention is being shifted toward this mechanical degradation mechanism as the next limiting factor in membrane lifetime. The

* Corresponding author. Tel.: +1 778 782 8791; fax: +1 778 782 7514.
E-mail address: ekjeang@sfu.ca (E. Kjeang).

0378-7753/$ – see front matter © 2013 Elsevier B.V. All rights reserved.
http://dx.doi.org/10.1016/j.jpowsour.2013.01.128

primary cause of hygrothermal stress within the membrane is its high propensity for water absorption, which results in considerable swelling or contraction while it is confined inside the relatively rigid membrane electrode assembly (MEA) [7]. Understanding the dimensional change and response to mechanical stresses is critical to addressing the mechanical durability issues.

Numerous studies have been conducted on the mechanical properties of PFSA membranes such as Nafion® as a function of temperature and/or relative humidity [5,8–17]. By means of *ex situ* characterization at controlled mechanical and environmental conditions, it was found that higher temperature and higher relative humidity both independently reduce the stiffness of PFSA membranes [5,9–15]. However, the interaction of temperature and humidity was not always considered. In a study by Bauer et al. [11], water was found to have a plasticizing effect at lower temperatures, whereas the presence of a small amount of water at higher temperatures tended to stiffen the membrane material. It was argued that the increased water content contributed more hydrogen bonding which had an observable stiffening effect relative to the more mobile polymer chains at high temperature. Similar results were also found in creep and stress relaxation experiments by Majsztrik et al. [14] and tensile experiments by Satterfield et al. [12,13], which both emphasized the need for carefully controlled environmental conditions. Given the high operating temperature and relative humidity inside a fuel cell, the first approach to address the mechanical durability issues is to increase the modulus of the membrane at these conditions. Membranes that have been mechanically reinforced with ePTFE fibers have achieved some of the longest lifetimes in accelerated durability tests [18].

The swelling of the membrane is another important factor to consider when seeking to improve durability. Directly related to the water content, the dimensional swelling and contraction of the membrane is the ultimate cause of the induced hygrothermal stresses which may eventually lead to mechanical fatigue. Defined as the number of water molecules per sulfonic acid group, λ has been shown to vary from 2 in desiccated conditions to as high as 22 for Nafion® membranes immersed in liquid water [19]. This level of sorption can translate to dimensional changes over 15% [20]. These observations have led to several modeling studies attempting to quantify the stresses which may be experienced by the membrane when confined between a gas diffusion layer (GDL) or flow field plates with much higher stiffness [21–25]. Several of these studies have demonstrated that the stresses induced by dimensional changes can be sufficient to cause significant stress and possibly permanent plastic deformation [22,25].

Characterizing the mechanical behavior of the PFSA materials which are most susceptible to mechanical degradation is a good starting point toward understanding the limiting factors of fuel cell lifetime. Inside a fuel cell membrane electrode assembly (MEA) however, the membrane is fused together with the anode and cathode catalyst layers on each side to form a catalyst coated membrane (CCM). The two catalyst layers contain ionomer of similar nature to that of the membrane and may therefore have an influence on the true *in situ* mechanical behavior of the membrane in a fuel cell. In contrast to previous studies exclusively considering the properties of pure membranes, the objective of the present work is to characterize a complete set of mechanical properties of a standard CCM and evaluate the differences compared to a sole membrane. A statistical design of experiments approach is employed to investigate static CCM mechanical properties under a range of temperature and relative humidity conditions representative of the operating environment in a fuel cell. The obtained properties are expected to be useful for accurate modeling of stress distributions within the MEA as well as for durability studies with respect to mechanical degradation of the CCM.

2. Experimental methods

2.1. Materials

The pure membranes used throughout this study were taken from a single batch of commercially available standard dispersion cast PFSA. To ensure consistency, rectangular samples were cut along the transverse direction even though no measurable difference in mechanical properties was observed for perpendicular directions upon initial screening. Samples were stored at room conditions for several days without any other form of conditioning prior to testing. Membrane electrode assemblies (MEA) manufactured from the same PFSA material using a proprietary method were provided by Ballard Power Systems. After delamination of the gas diffusion layers, the remaining catalyst coated membranes were then cut into similar strips and stored at the same conditions. Sample widths were measured via optical microscope and thicknesses with a digital micrometer. The CCM samples were imaged by optical microscope both prior to and after testing to screen any samples with defects.

2.2. Apparatus & sample loading

A dynamic mechanical analyzer (TA Instruments Q800 DMA) equipped with an environmental chamber (TA Instruments DMA-RH Accessory) was used for all measurements. Tensile test samples were loaded in a film tension clamp with a length to width aspect ratio of 5:1, which was determined experimentally beforehand to be adequate to avoid any edge or stress concentration effects for PFSA materials. The samples seldom fractured within the displacement range of the clamp fixture, which is the reason why fracture strain and ultimate stress values are not considered in this study. Samples were loaded at room conditions and brought to the desired environmental conditions and allowed to equilibrate with a minimal preload force being applied to keep the sample in tension. The sample length was monitored and the tensile test was started when the swelling due to heating and water absorption stabilized to less than 1 μm min^{-1}.

2.3. Procedure & conditions

Dynamic mechanical analysis was performed to study the transition phenomena of the membrane and CCM specimens as a function of temperature. Samples were loaded in the standard DMA furnace at a gauge length of approximately 10 mm and allowed to equilibrate before being tested at a frequency of 1 Hz while the temperature was increased at a rate of 2 °C min^{-1}.

The core of the present study consists of constant strain rate tensile tests which follow a 2^2 factorial experimental design. The two factors, temperature and relative humidity, are varied jointly across a range of relevant fuel cell conditions in order to estimate main effects and interaction effects. Standard fuel cell operating conditions at 70 °C, 90% RH and room conditions at 23 °C, 50% RH make up the two extreme corners of the experiment, while 70 °C, 50% RH and 23 °C, 90% RH make up the remaining corners. Center points at 47 °C, 70% RH were also included to test for non-linear behavior which is referred to as curvature. Four samples of pure membrane and four samples of CCM were tested at each corner. The results presented in this study were measured using a 0.01 min^{-1} engineering strain rate, and were also repeated at a strain rate of 0.1 min^{-1} to provide additional verification of observed behavior. The effects of temperature and humidity are discerned by comparing the means at each experimental corner with a standard *F-test* analysis of variance (ANOVA) statistical method.

A series of isostrain and isoforce tests were conducted to determine whether the tensile stresses generated during membrane and

CCM dehydration were equivalent. For isostrain tests, identical width samples were loaded at the same length and allowed to equilibrate at the set conditions under a minimal preload force. Upon equilibration, samples were kept at a nominal strain of 0.1% to simulate confinement within a fuel cell, while the relative humidity was decreased and the contraction force was measured. Isoforce tests were conducted in the same manner with the exception that a constant force of 0.01 N was applied to the samples while the relative humidity was decreased and the contraction strain was measured.

2.4. Definitions

In this study, all values refer to the directly measured engineering stress σ and engineering strain ε, and all error bars indicate ± 2 standard deviations. Often defined as the elastic or Young's modulus in the literature, the initial tangent modulus of the curve was determined from the maximum slope of a 5th order polynomial fit to the initial section between 0 and 0.5% strain. This method avoids any human subjectivity while being robust to any remaining toe region due to an insufficient preload force. Given that the strain rates used are not appropriate for measuring purely elastic properties of the polymer at all environmental conditions the initial tangent modulus which still reflects the stiffness of the materials, is simply referred to as modulus from this point onward. Two methods were used to define the onset of yielding behavior, the first being the offset yield as suggested in the ASTM D882 standard [26], and the second being the proportional limit yield more commonly used in the literature related to these materials [10,21]. For the sake of brevity, the yielding behavior captured by these methods is interchangeably referred to as yield stress throughout this work.

3. Results & discussion

In order to compare the mechanical properties of two materials, one pure polymer and the other a composite based on the same polymer, it was decided to start with dynamic measurements of the polymer structure. These preliminary tests were followed by a systematic study of the tensile properties of both materials as a function of temperature and humidity. This study was then concluded with a comparison of dimensional changes experienced by both materials due to variation in humidity.

3.1. Transition temperature

Before undertaking systematic investigations into the standard mechanical properties of the materials considered, it is logical to check whether the CCM fabrication process might fundamentally change the membrane material. Directly related to the length of the polymer chains and the presence of any crystallized domains, transition phenomena can be measured by dynamic mechanical analysis. Some of the first measurements of transition temperatures for PFSA were conducted by Yeo and Eisenberg in 1977 [27]. In that study, it was found that the material exhibits transition behavior around 110 °C. Other studies, such as those by Bauer et al. [11] have looked more carefully at the humidity dependence of these phenomena. Often referred to as the α-transition, a sudden decrease in the storage modulus of the material between 80 and 100 °C indicates the disintegration of the crystallized domains into an amorphous network. The inflection point in the storage modulus typically coincides with a peak in tan δ, which is the more commonly used definition for the transition. The data shown in Fig. 1 displays the peaks in tan δ for the membrane and the CCM. The peak for this PFSA material lies roughly around 91 °C, which is lower than the values found in the literature for similar materials, but scan rate and pretreatment have both been shown to affect the location of the peak [8]. If any significant changes to the polymer molecules or network of the membrane occurred during fabrication, we would expect to see a shift in the transition temperature. Moreover, if any substantial amount of other polymers were present in the catalyst layers, secondary peaks might also be detected. Neither case occurs for the CCM, which confirms that the fabrication process did not have a measurable impact on the polymeric structure of the membrane within the CCM.

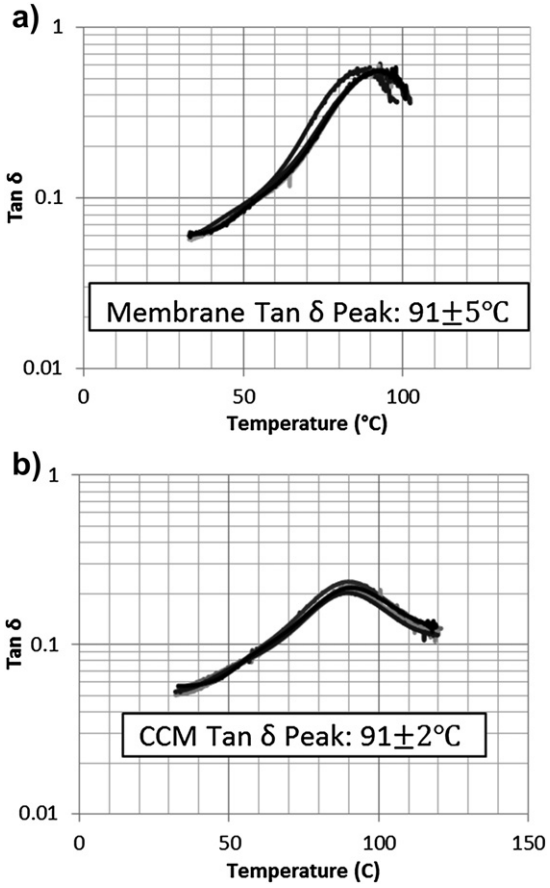

Fig. 1. Comparison between tan δ peaks for four PFSA membrane replicates (a) and four CCM replicates (b).

3.2. Factorial study of tensile behavior

The purpose of the present factorial study is to quantify the effects that temperature and humidity have on the mechanical properties of both the membrane and CCM. Statistical analysis of the results will reveal whether any significant trends can be associated with the variation of these environmental factors. Before discussing the full results of this study, the high sensitivity of PFSA to both humidity and temperature can immediately be seen from qualitative and quantitative differences of the stress–strain curves shown in Fig. 2. When assessing the mechanical properties of a material it is necessary to normalize the force measurement by the cross-sectional area of the sample to obtain these stress values. For the PFSA membrane the typical method found in the literature has been to use the relatively uniform thickness provided by the manufacturer and the measured width of the samples. For the composite CCM materials, however, there are two alternative approaches. The first option is to consider the membrane to be the

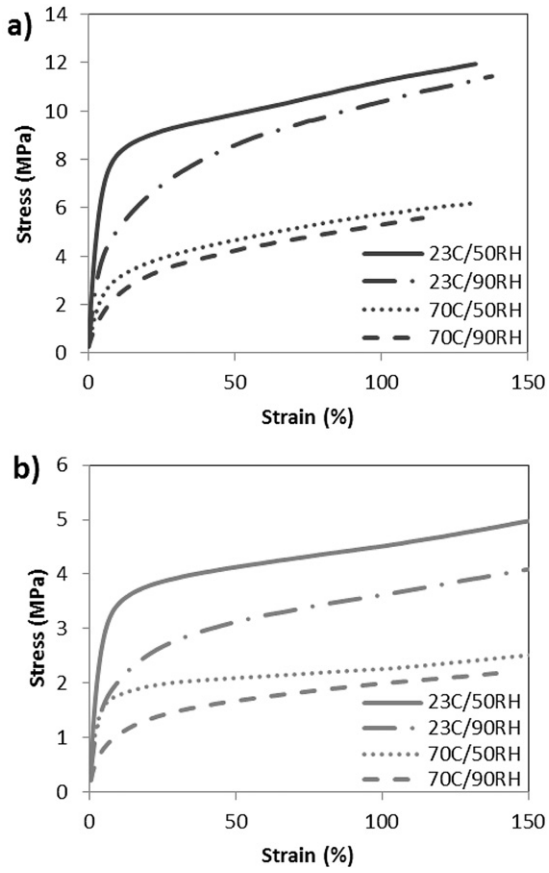

Fig. 2. Example stress–strain curves for PFSA membrane (a), and CCM (b).

only load bearing structure and normalize the stress according to the membrane thickness [5,6]. The second option is to measure the thickness of each CCM sample individually and apply a heterogeneous normalization [9]. In the present study, the second approach is chosen based on the treatment of the CCM as a composite structure with bonded ionomer in all three layers. It may be surprising that the loosely constructed and highly porous catalyst layer would offer any mechanical support to the CCM but as the example data in Fig. 3 shows, this is indeed the case. For two samples of equal length and width, in identical environmental conditions, the CCM strip resists the same deformation with more force. Although the CCM strip is a stronger object, when normalized by the measured thickness of each sample, the composite material yields more easily than pure PFSA material which can be seen in the example stress versus strain curves of Fig. 2.

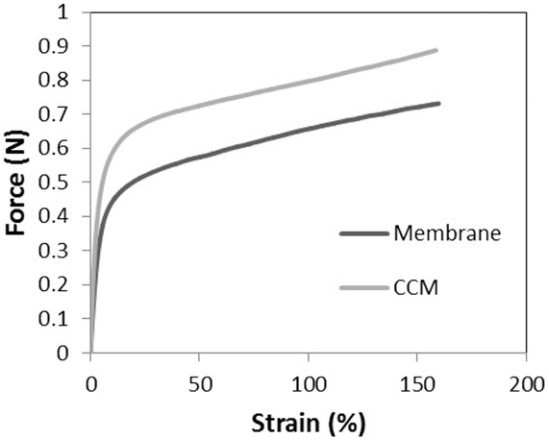

Fig. 3. Comparison of force vs. strain for PFSA membrane (bottom curve) and CCM (top curve) at room conditions.

3.2.1. Modulus

The data presented in Fig. 4 shows the average initial modulus calculated from the stress–strain curves for both membrane and CCM measured at the selected combinations of temperature, relative humidity, and strain rate. As explained previously, it is clear from the lower modulus values that the CCM material, when normalized by its measured thickness, is comparatively less stiff than pure PFSA at all tested environmental conditions; i.e., the membrane is the stiffest part of the CCM while the catalyst layers contribute a lower level of additional reinforcement. The results of the ANOVA, which was conducted in order to quantify the effects of temperature and relative humidity on the modulus of these materials, are summarized in Tables 1 and 2. In agreement with the literature, an increase in either temperature or RH has a negative effect on the modulus of the PFSA material, regardless of strain rate. In contrast, the interaction between temperature and RH seems to have a positive effect on the modulus. This can be associated with

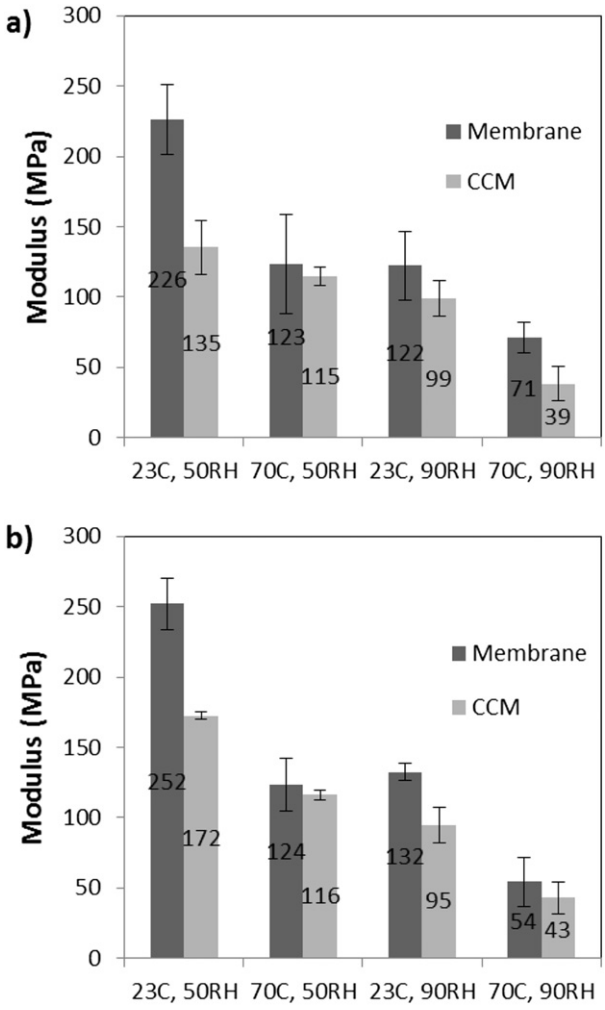

Fig. 4. Variation of initial modulus as a function of environmental conditions for both PFSA membrane (left columns) and CCM (right columns). Strain rate 0.01 min^{-1} (a), and 0.1 min^{-1} (b).

Table 1
ANOVA of modulus results for 0.01 min^{-1} strain rate.

Factor	Membrane		CCM	
	Effect (MPa)	*P* value	Effect (MPa)	*P* value
Temperature	−77	<0.0001	−40	<0.0001
Relative humidity	−78	<0.0001	−56	<0.0001
Interaction	26	0.0016	−20	0.0003

the presence of water which tends to add stiffness to the membrane at higher temperatures [11].

The measured modulus of the CCM exhibits similar trends to that of the pure PFSA material but with relatively diminished effects. For both the CCM and membrane, the humidity and temperature independently have negative main effects of similar magnitude. However, an important distinction is found in the obtained interaction effect, which is negative at the lower strain rate and statistically insignificant at the higher strain rate. We focus here on the lower strain rate due to the higher accuracy and more realistic behavior in the context of fuel cell operation. Interestingly, in contrast to the result for the bare membrane, the combined effect of high humidity and high temperature appears to have a softening effect on the overall CCM object. Furthermore, the results of the statistical curvature tests (not shown here) indicate that the modulus of both the membrane and CCM vary nonlinearly with temperature and relative humidity. According to the basic laminar composite theory [28], the modulus of the laminate is simply obtained by adding the moduli of the separate layers according to their relative thicknesses:

$$E_{comp}t_{comp} = E_1t_1 + E_2t_2 + E_3t_3 + \cdots \quad (1)$$

where E_n and t_n are the modulus and thickness of each layer respectively. Consequently, magnified trends would be expected by increasing the thickness of the catalyst layers.

3.2.2. Yield stress

The data in Fig. 5 displays the average yield stress computed from the stress–strain curves for all test conditions and the ANOVA for these results is presented in Tables 3 and 4. All values are based on the proportional limit stress as defined previously; however, the 2% offset yield stress method is found to produce the same general trends. Similarly to the modulus results, an increase in the main effects of temperature or humidity tends to decrease the yield stress for the PFSA material. This is in good agreement with previous work by Tang et al. [10] on PFSA membranes. In accordance with the Satterfield et al. study on Nafion® [12], the results also show that the interaction of high temperature and high humidity adds a positive or strengthening interaction effect. Again, there is an indication of curvature for the pure PFSA material with respect to temperature and RH due to the average yield stress at the center point of the experimental design being larger than the average of the four corners (not shown here).

For the CCM case, the variation in yield stress follows the same general trends with only a few minor differences. The interaction

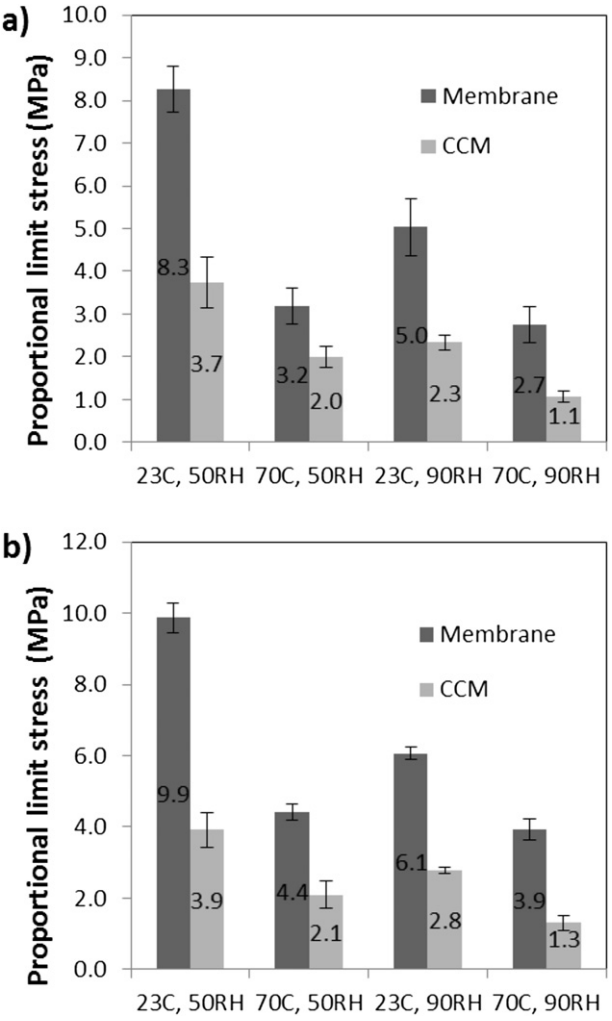

Fig. 5. Variation of proportional limit stress as a function of environmental conditions for both PFSA membrane (left columns) and CCM (right columns). Strain rate 0.01 min^{-1} (a), and 0.1 min^{-1} (b).

effect is considerably smaller relative to the main effects, having a relative magnitude of only 20% of the RH effect, whereas it was over 50% for the PFSA case. As in this example, comparisons between relative magnitudes of the effects are more meaningful for both the modulus and yield stress since these are directly related to the different thicknesses of the materials. One exception to this is the effect of temperature which is noticeably reduced for the CCM compared to the membrane. No curvature was observed for the yield stress of the CCM.

3.2.3. Yield strain

Looking back at the stress–strain curves in Fig. 2 it can be seen that the yield strain is less distinctly defined due to the variation in curve shape. The definition of the initial modulus as the maximum

Table 2
ANOVA of modulus results for 0.1 min^{-1} strain rate.

Factor	Membrane		CCM	
	Effect (MPa)	*P* value	Effect (MPa)	*P* value
Temperature	−103	<0.0001	−54	<0.0001
Relative humidity	−94	<0.0001	−75	<0.0001
Interaction	25	<0.0001	2	0.34

Table 3
ANOVA of proportional limit stress results for 0.01 min^{-1} strain rate.

Factor	Membrane		CCM	
	Effect (MPa)	*P* value	Effect (MPa)	*P* value
Temperature	−3.7	<0.0001	−1.5	<0.0001
Relative humidity	−1.8	<0.0001	−1.2	<0.0001
Interaction	1.4	<0.0001	0.2	0.01

Table 4
ANOVA of proportional limit stress results for 0.1 min^{-1} strain rate.

Factor	Membrane		CCM	
	Effect (MPa)	*P* value	Effect (MPa)	*P* value
Temperature	−3.8	<0.0001	−1.6	<0.0001
Relative humidity	−2.1	<0.0001	−1.0	<0.0001
Interaction	1.7	<0.0001	0.2	0.07

Table 5
ANOVA of proportional limit strain results for 0.01 min^{-1} strain rate.

Factor	Membrane		CCM	
	Effect (%)	*P* value	Effect (%)	*P* value
Temperature	−0.8	<0.0001	−0.4	0.0041
Relative humidity	0.8	0.0002	0.3	0.0170
Interaction	0.4	0.0260	0.7	<0.0001

slope is unambiguous, whereas the definition of the yield point is dependent on which method is chosen. Regardless of the method, if the differences are pronounced enough, as for the yield stress, the analysis should reveal the appropriate relationships. In this case, the differences in yield strain are small compared to the bias introduced by the offset method which consequently fails to capture some of the observable trends. Using the preferred proportional limit method, the average yield strains are collected in Fig. 6 with the corresponding ANOVA results provided in Tables 5 and 6. Although all effects have statistical significance, the trends are not as clear in this case as for the modulus or stress. For the pure membrane there is drastic change in behavior between low and high strain rate which would suggest that the strain rate should be considered as a third factor. The data are therefore also analyzed as a three-factor ANOVA (not shown here) and the effect of strain rate

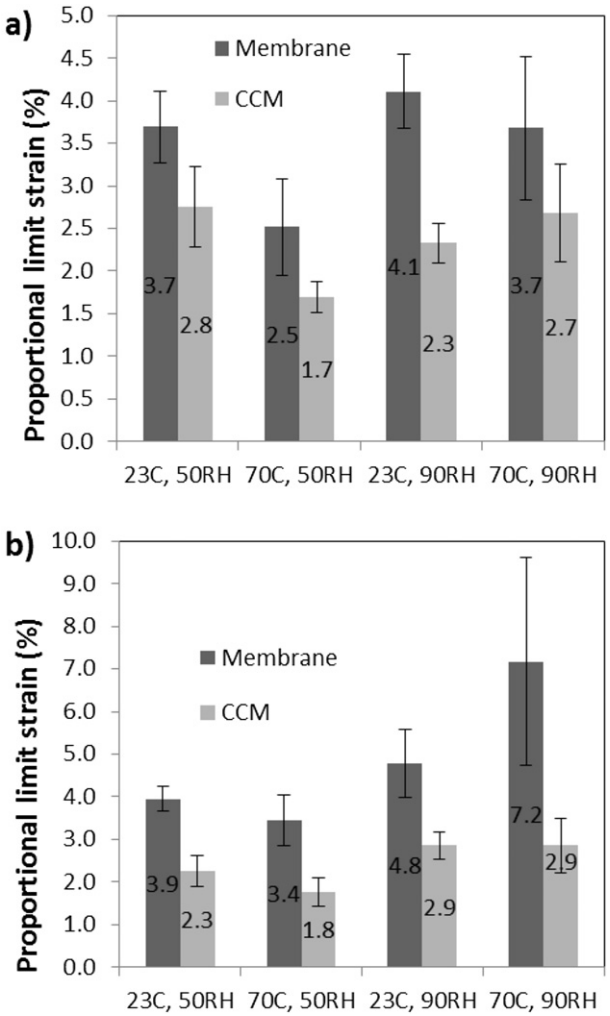

Fig. 6. Variation of proportional limit strain as a function of environmental conditions for both PFSA membrane (left columns) and CCM (right columns). Strain rate 0.01 min^{-1} (a), and 0.1 min^{-1} (b).

is determined to be stronger than the effects of the environmental conditions, generally increasing the yield strain at a higher rate. This observation is supported by the data presented in Satterfield's thesis which also showed a positive relationship between yield strain and strain rate. The positive relationship between relative humidity and yield strain seen here is also indicated in that study [13]. When analyzed as a three-factor experiment, the temperature is shown to have little effect, which suggests that the temperature effects indicated here may be masked by the strain rate. The CCM behavior on the other hand shows little dependence on the strain rate when analyzed as a three-factor experimental design whereas the positive effect of humidity seen for PFSA is still present in the CCM. Comparatively less data on the yield strain of PFSA is available in the literature and as such the physical interpretation for these effects is more difficult to understand.

The most meaningful relationship to extract from the yield strain data however is the overall difference between the CCM and pure membrane. All samples were loaded at roughly the same length and therefore can be compared directly in terms of strain magnitude. From Fig. 6 it is apparent that the CCM yields before the pure membrane at all environmental conditions. It is often understood that the catalyst layers are more brittle than the underlying membrane, a point which is clearly visible in the microscope image of a post-test CCM shown in Fig. 7. Although the catalyst layers tend to disintegrate and crack gradually as the samples are stretched, once the membrane begins to yield, the fragmentation becomes significant enough for the underlying membrane to become the major load bearing structure. One way to verify this assertion is by looking back at Fig. 3. When plotted in terms of force, both the CCM and membrane samples of the same width will have the exact same slope after the yield point. The constant bias present in the plastic region indicates that residual stress remains in the catalyst layers of the CCM attached to the membrane even after they have yielded and therefore they continue to offer some structural support. An important study by Pestrak et al. demonstrated that catalyst coated membranes may have shorter lifetimes than uncoated membranes due to the pressure concentration at cracks in the catalyst layer [29]. The results observed here seem to support this idea and suggest that current efforts being made to reinforce the membrane should not neglect the integrity of the catalyst layers. It is possible that mechanically induced deformation and fractures are formed in the catalyst layers at relatively low levels of stress and strain, and may potentially propagate into the membrane.

3.2.4. Summary of environmental effects

The trends observed throughout the factorial study can be succinctly visualized with the interaction plots in Fig. 8. For the

Table 6
ANOVA of proportional limit strain results for 0.1 min^{-1} strain rate.

Factor	Membrane		CCM	
	Effect (%)	*P* value	Effect (%)	*P* value
Temperature	0.9	0.0150	−0.2	0.0440
Relative humidity	2.3	<0.0001	0.8	<0.0001
Interaction	1.4	0.0009	0.2	0.0440

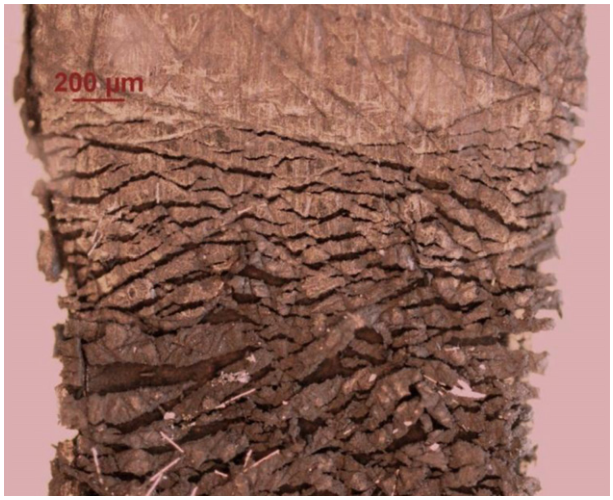

Fig. 7. Optical microscope image of a CCM sample after tensile test.

most part, the effects are similar at both strain rates but only the 0.01 min^{-1} strain rate is shown since it generally has more statistical significance and is likely more relevant to the applied stresses during hygrothermal loading. The slope of the lines indicates the magnitude and direction of the effects, whereas the interaction effect is represented by the parallelism of the lines. As mentioned previously, the temperature and humidity tend to have similar effects on both the CCM and membrane. The CCM yield stress lines are more parallel however because the interaction effects are reduced, whereas the modulus lines converge in the PFSA case and diverge for the CCM. In practical terms, this means that the decrease in both stiffness and yielding of the CCM is proportionally more pronounced at standard fuel cell operating conditions (70 °C, 90% RH) than it is for the pure PFSA membrane.

Considering the fact that membrane and catalyst layer thicknesses are typically selected based on higher priority needs directly related to fuel cell performance and cost, it may be enlightening to look at the mechanical properties of both objects without normalizing by the thickness. By extracting the measured thickness of each sample from the modulus and yield stress calculations it is possible to understand how a unit *width* of either object will resist

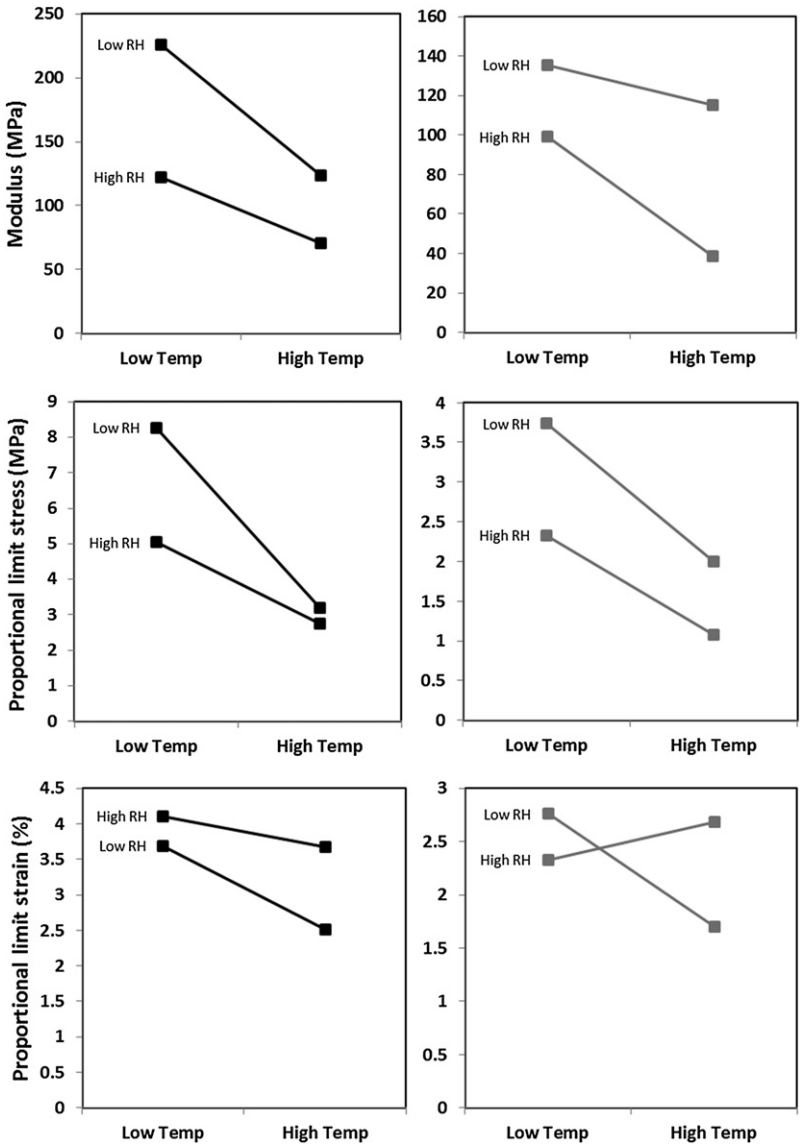

Fig. 8. Interaction plots for PFSA membrane (left) and CCM (right) at a 0.01 min^{-1} strain rate. Low RH = 50%, high RH = 90%, low Temp = 23 °C, high Temp = 70 °C.

an applied force. A direct comparison can then be made on the effects of temperature and humidity on the effective stiffness (defined here as 'modulus by width') and strength (defined here as 'limit stress by width') of each *strip* of material, as illustrated in Fig. 9. These results demonstrate the same behavior indicated in Fig. 2, namely that a piece of CCM of the same width will resist more strongly to an applied force than a membrane. In this case, however, it can be seen more directly that the reinforcement provided by the catalyst layers is in itself a function of temperature and humidity. These results reflect the trends seen in the factorial ANOVA. For instance, the lower relative effect of temperature on modulus seen for CCM in Table 1 can be observed again here. An ANOVA conducted on the data with the thickness extracted as in Fig. 9 reveals the same general trends and statistical significance seen for the modulus and limit stress as typically defined. This indicates that the added variability due to the thickness measurement is minor compared to the effect of environmental conditions. This type of simplification is not possible when attempting to model the stress distribution inside the MEA however, and would require more knowledge of the effective cross-sectional area of the catalyst layers. As seen in the following section, the effects observed in this factorial study may be due to the differences in water absorption between the membrane and CCM.

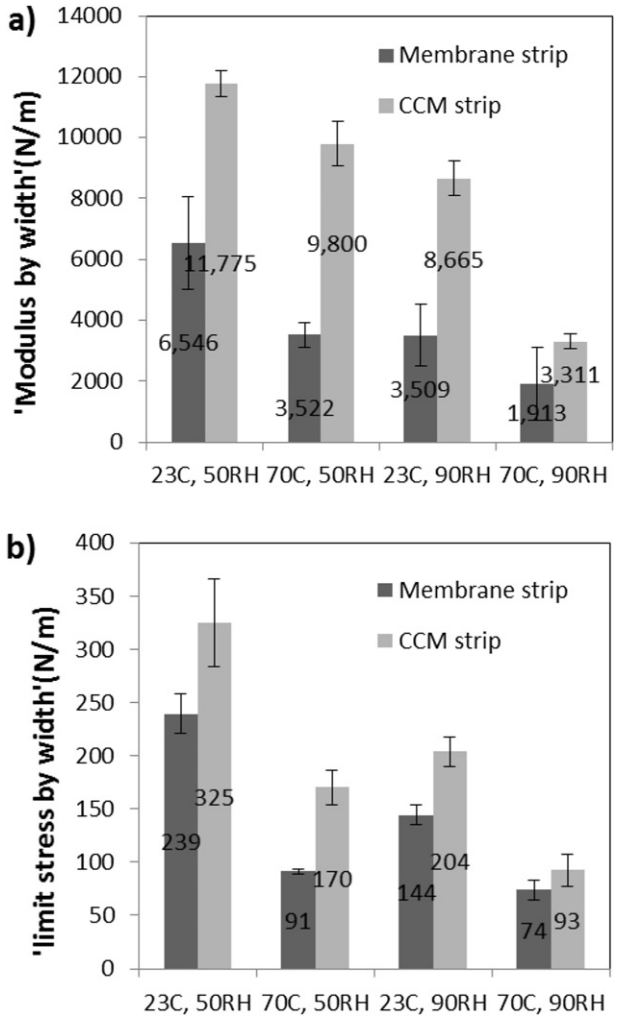

Fig. 9. Comparison of effective mechanical behavior of membrane (left columns) and CCM (right columns) objects as a function of environmental conditions. Strain rate 0.01 min^{-1}. Width normalized modulus (a), width normalized proportional limit stress (b).

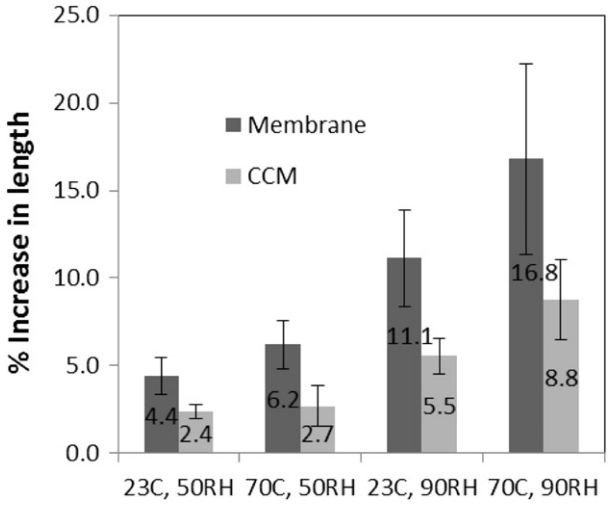

Fig. 10. Increase in length during equilibration of samples at environmental conditions. PFSA membrane (left columns) and CCM (right columns) are compared.

3.3. Swelling and contraction measurements

After studying the CCM's response to stress at varying environmental conditions, it is essential to understand how these stresses are actually created inside an operating fuel cell. For this purpose, the change in length of all samples used in the tensile tests when brought from ambient conditions to test conditions is monitored until a sufficient state of equilibrium is reached. These dimensional changes are summarized in Fig. 10 and demonstrate that at all environmental conditions, the length-wise swelling of the pure PFSA membrane is almost twice that of the CCM. Possibly due to the reinforcement provided by the catalyst layers and the composite nature of the CCM, this difference is of crucial importance when attempting to construct accurate models of mechanical degradation. As an additional step to verify whether these differences are present during dehydration, more samples were brought to elevated environmental conditions, allowed to equilibrate, measured in length while humidified, and then dehydrated back to room conditions under a constant minimal force while the strain is observed. Fig. 11 shows an example of such a test which adds further evidence of the same smaller dimensional change of the CCM versus the membrane.

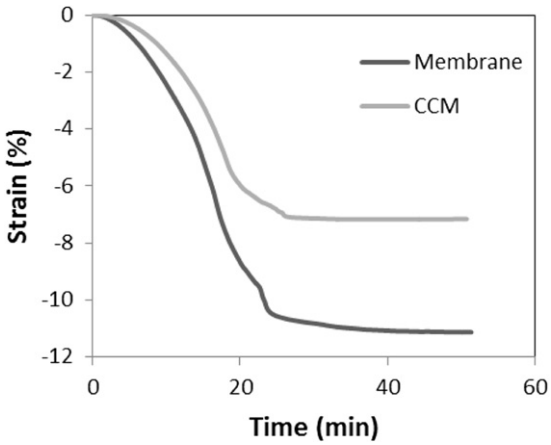

Fig. 11. Example of contraction due to dehydration for PFSA membrane (bottom curve) and CCM (top curve). Test conditions: Relative humidity dropping from 90% to 50% at 70 °C.

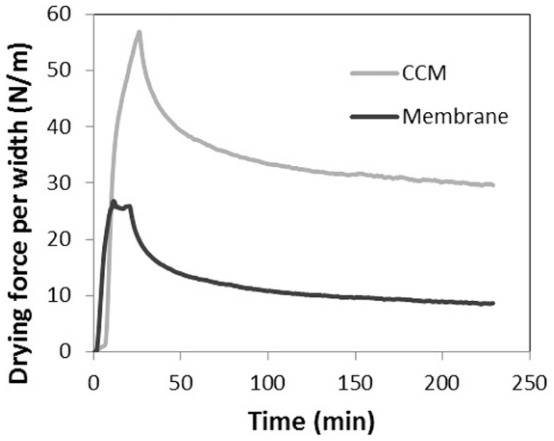

Fig. 12. Example of force per unit width due to dehydration of samples during isostrain confinement for PFSA membrane (top curve) and CCM (bottom curve). Test conditions: Relative humidity dropping from 90% to 50% at 70 °C.

Similarly, the stress induced by the drying samples can also be monitored during isostrain tests. Fig. 12 shows the drying force produced by identical width samples at the same test conditions as in Fig. 11. In this case, the CCM produces more than twice as much peak dehydration force as the PFSA membrane and more than three times the residual force after 200 min of equilibration. The repercussions of these differences are clear when looking back at Fig. 9. Although the 'modulus by width' is always higher for the CCM than for the membrane, the reinforcement provided by the catalyst layers may not outweigh the increase in residual tensile dehydration force that they cause. These results indicate that more attention to such details is required to adequately understand the mechanical behavior of the CCM when situated inside a fuel cell. Correlating the tensile properties with the dimensional changes and the forces created by these dimensional changes is the most crucial goal for modeling of stress distributions within an MEA.

4. Conclusions

The mechanical properties of a catalyst coated PFSA membrane have been measured as a function of humidity and temperature and compared to those of a pure PFSA membrane at the same conditions. Although the results from dynamic measurements indicate no change in the length of the polymer chains during catalyst layer bonding, the results from the tensile measurements indicate several differences in mechanical behavior between the two materials. In general, the CCM material yields at lower strain values than the pure membrane material. An increase in temperature or an increase in relative humidity both reduce the modulus and yield stress of the membrane and CCM, whereas the interaction effect between the temperature and humidity seems to have a positive effect on the membrane but not the CCM. The relative degree of these effects varies significantly between each material, with the end result that the overall mechanical strength and stiffness of the CCM have decreased more than the membrane at operating fuel cell conditions (70 °C, 90% RH) as compared to room conditions.

The swelling and contraction properties of the two materials were also investigated with respect to relative humidity. The swelling of the materials during equilibration was monitored at all environmental conditions under study. It was found that on average the percent increase in length of the membrane samples was almost twice as high as for CCM. This ratio was also observed upon dehydration, with the membrane contracting nearly twice as much. Isostrain tests were also conducted to measure the forces created by this dehydration and it was found that both the peak and residual forces are greater for the CCM during dehydration than for the membrane. When compared to the differences in yield and stiffness between these two materials measured during tensile tests, the dehydration forces indicate that the mechanical reinforcement in the tensile direction provided by the catalyst layers of the CCM does not always outweigh the increase in dehydration force caused by them.

The relationships observed in these experiments demonstrate that the mechanical properties of the CCM vary differently than those of the membrane with respect to temperature and humidity. For this reason, *in situ* mechanical models of membrane stress distributions are unlikely to correlate directly with the true distributions experienced by the catalyst coated membrane within a fuel cell. The data gathered as part of this study will become useful as part of an empirical model of mechanical properties of CCM as a function of environmental conditions. More environmental conditions can be included in the future to accurately assess the degree of curvature and obtain a more precise understanding of the influence of temperature and humidity on the CCM.

Acknowledgments

Funding for this research provided by the Automotive Partnership Canada (APC), Ballard Power Systems, and Simon Fraser University is highly appreciated. We are indebted to Chan Lim, Jeffrey To, Stephan Rayner, and Jeetinder Ghataurah at SFU and Warren Williams at Ballard for their assistance in experimentation. We also acknowledge Ballard Power Systems for providing material samples.

References

[1] K.A. Mauritz, R.B. Moore, Chemical Reviews 104 (2004) 4535–4586.
[2] R. Borup, J. Meyers, B. Pivovar, Y.S. Kim, R. Mukundan, N. Garland, D. Myers, M. Wilson, F. Garzon, D. Wood, P. Zelenay, K. More, K. Stroh, T. Zawodzinski, J. Boncella, J.E. McGrath, M. Inaba, K. Miyatake, M. Hori, K. Ota, Z. Ogumi, S. Miyata, A. Nishikata, Z. Siroma, Y. Uchimoto, K. Yasuda, K. Kimijima, N. Iwashita, Chemical Reviews 107 (2007) 3904–3951.
[3] J. Wu, X.Z. Yuan, J.J. Martin, H. Wang, J. Zhang, J. Shen, S. Wua, W. Merida, Journal of Power Sources 184 (2008) 104–119.
[4] Y.-H. Lai, C.S. Gittleman, C.K. Mittelsteadt, D.A. Dillard, in: Proceedings of the 3rd International Conference on Fuel Cell Science, Engineering, and Technology, Ypsilanti, MI, United States, 2005, pp. 161–167.
[5] X. Huang, R. Solasi, Y. Zou, M. Feshler, K. Reifsnider, D. Condit, S. Burlatsky, T. Madden, Journal of Polymer Science Part B Polymer Physics 44 (2006) 2346–2357.
[6] T.T. Aindow, J. O'Neill, Journal of Power Sources 196 (2011) 3851–3854.
[7] Y.-H. Lai, C.K. Mittelsteadt, C.S. Gittleman, D.A. Dillard, Journal of Fuel Cell Science and Technology 6 (2009) 021002.
[8] J.T. Uan-Zo-li, The Effects of Structure, Humidity and Aging on the Mechanical Properties of Polymeric Ionomers for Fuel Cell Applications, Master thesis, Virginia Tech, 2001.
[9] S. Kundu, L.C. Simon, M. Fowler, S. Grot, Polymer 46 (2005) 11707–11715.
[10] Y. Tang, A.M. Karlsson, M.H. Santare, M. Gilbert, S. Cleghorn, W.B. Johnson, Material Science and Engineering A 425 (2006) 297–304.
[11] F. Bauer, S. Denneler, M. Willert-Porada, Journal of Polymer Science Part B Polymer Physics 43 (2005) 786–795.
[12] M.B. Satterfield, P.W. Majsztrik, H. Ota, J.B. Benziger, A.B. Bocarsly, Journal of Polymer Science Part B Polymer Physics 44 (2006) 2327–2345.
[13] M.B. Satterfield, Mechanical and Water Sorption Properties of Nafion and Composite Nafion/Titanium Dioxide Membranes for Polymer Electrolyte Membrane, Dissertation, Chemical Engineering Department, Princeton University, Princeton, NJ, 2007.
[14] P.W. Majsztrik, A.B. Bocarsly, J.B. Benziger, Macromolecules 41 (2008) 9849–9862.
[15] M.N. Silberstein, M.C. Boyce, Journal of Power Sources 196 (2011) 3452–3460.
[16] R. Solasi, X. Huang, K. Reifsnider, Mechanics of Materials 42 (2010) 678–685.
[17] Y. Li, D. a. Dillard, Y.-H. Lai, S.W. Case, M.W. Ellis, M.K. Budinski, C.S. Gittleman, Journal of The Electrochemical Society 159 (2012) B173.
[18] M. Crum, W. Liu, ECS Transactions 3 (2006) 541–550.
[19] P. Choi, N.H. Jalani, T.M. Thampan, R. Datta, Journal of Polymer Science Part B Polymer Physics 44 (2006) 2183–2200.
[20] J. Peron, A. Mani, X. Zhao, D. Edwards, M. Adachi, T. Soboleva, Z. Shi, Z. Xie, T. Navessin, S. Holdcroft, Journal of Membrane Science 356 (2010) 44–51.
[21] M.N. Silberstein, M.C. Boyce, Journal of Power Sources 195 (2010) 5692–5706.

[22] A. Kusoglu, A.M. Karlsson, M.H. Santare, S. Cleghorn, W.B. Johnson, Journal of Power Sources 161 (2006) 987–996.
[23] A. Kusoglu, A.M. Karlsson, M.H. Santare, S. Cleghorn, W.B. Johnson, Journal of Power Sources 170 (2007) 345–358.
[24] Z. Lu, C. Kim, A.M. Karlsson, J.C. Cross, M.H. Santare, Journal of Power Sources 196 (2011) 4646–4654.
[25] R. Solasi, Y. Zou, X. Huang, K. Reifsnider, D. Condit, Journal of Power Sources 167 (2007) 366–377.
[26] ASTM, D882-10 Standard Test Method for Tensile Properties of Thin Plastic Sheeting, 2011, pp. 1–10.
[27] S.C. Yeo, A. Eisenberg, Journal of Applied Polymer Science 21 (1977) 875–898.
[28] D.F. Adams, L.A. Carlsson, R.B. Pipes, Experimental Characterization of Advanced Composite Materials, CRC Press, New York, 2003.
[29] M. Pestrak, Y. Li, S.W. Case, D. a. Dillard, M.W. Ellis, Y.-H. Lai, C.S. Gittleman, Journal of Fuel Cell Science and Technology 7 (2010) 041009.